JACS
JOURNAL OF THE AMERICAN CHEMICAL SOCIETY

Subscriber access provided by ISTANBUL TEKNIK UNIV

Article

Boron Rings Enclosing Planar Hypercoordinate Group 14 Elements

Rafael Islas, Thomas Heine, Keigo Ito, Paul v. R. Schleyer, and Gabriel Merino

J. Am. Chem. Soc., **2007**, 129 (47), 14767-14774 • DOI: 10.1021/ja074956m

Downloaded from http://pubs.acs.org on February 9, 2009

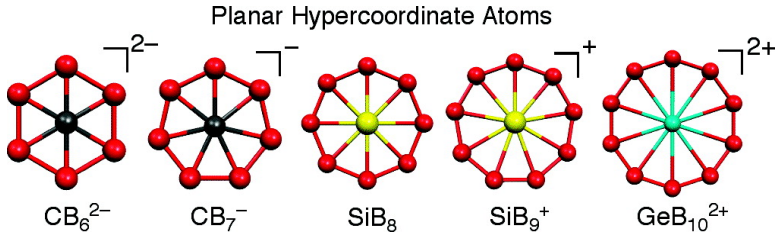

More About This Article

Additional resources and features associated with this article are available within the HTML version:

- Supporting Information
- Links to the 12 articles that cite this article, as of the time of this article download
- Access to high resolution figures
- Links to articles and content related to this article
- Copyright permission to reproduce figures and/or text from this article

View the Full Text HTML

ACS Publications
High quality. High impact.

Journal of the American Chemical Society is published by the American Chemical Society. 1155 Sixteenth Street N.W., Washington, DC 20036

J|A|C|S
ARTICLES
Published on Web 11/06/2007

Boron Rings Enclosing Planar Hypercoordinate Group 14 Elements

Rafael Islas,[†,‡] Thomas Heine,[‡] Keigo Ito,[§] Paul v. R. Schleyer,[§] and Gabriel Merino*,[†]

Contribution from the Facultad de Química, Universidad de Guanajuato. Col. Noria Alta s/n C.P. 36050, Guanajuato, Gto., México, Physikalische Chemie, Fachbereich Chemie, TU Dresden, D-01062 Dresden, Germany, Center for Computational Chemistry, University of Georgia, Athens, Georgia 30602-2525

Received July 31, 2007; E-mail: gmerino@quijote.ugto.mx

Abstract: Sets of boron rings enclosing planar hypercoordinate group 14 elements ($AB_n^{(n-8)}$; A = group 14 element; $n = 6-10$) are designed systematically based on geometrical and electronic fit principles: the size of a boron ring must accommodate the central atom comfortably. The electronic structures of the planar minima with hypercoordinate group 14 elements are doubly aromatic with six π and six in-plane radial MO systems (radial MOs are comprised of boron p orbitals pointing toward the ring center). This is confirmed by induced magnetic field and nucleus-independent chemical shift (NICS) computations. The weakness of the "partial" A−B bonds is compensated by their unusually large number. Although a C_{7v} pyramidal SiB_8 structure is more stable than the D_{8h} isomer, Born−Oppenheimer molecular dynamics simulations show the resistance of the D_{8h} local minimum against deformation and isomerization. Such evidence of the viability of the boron ring minima with group 14 elements encourages experimental realization.

I. Introduction

Molecules with non-classical bonding patterns, such as those with planar hypercoordinate elements, excite attention.[1−7] Monkhorst's 1968 computation of planar D_{4h} methane was the first theoretical investigation of a planar tetracoordinate carbon (ptC) configuration. Its extremely high energy precludes methane stereomutation.[8] In 1970, Hoffmann, Alder, and Wilcox suggested ways to reduce the strain energies of ptC molecules.[9] Collins et al.'s systematic computational investigation identified the first molecules with ptC minima in 1976.[10] The first experimental example of a ptC was reported by Cotton and Millar in 1977,[11] but the authors did not recognize their achievement at the time.[12]

The many subsequent theoretical and experimental investigations of ptC molecules have inspired the quest for systems containing planar carbon[13−38] with even higher coordination.[39−48] In 2000, Exner and Schleyer[39] and Minyaev and Gribanova[49] independently predicted the viability of several planar hexacoordinate carbon molecules with six π electrons. A year later, Wang and Schleyer reported building principles for generating a host of planar pentacoordinate carbon derivatives[41] and pointed out that CB_7^- (with a planar heptacoordinate carbon) was a minimum, also with six π electrons. They found that the next member of the six π electron series, neutral CB_8, does not have a planar octacoordinate carbon minimum; the carbon atom is

† Universidad de Guanajuato.
‡ TU Dresden.
§ University of Georgia.

(1) Sorger, K.; Schleyer, P. v. R. *THEOCHEM−J. Mol. Struct.* **1995**, *338*, 317.
(2) Rottger, D.; Erker, G. *Angew. Chem., Int. Ed.* **1997**, *36*, 813.
(3) Minkin, V. I.; Minyaev, R. M.; Hoffmann, R. *Usp. Khim.* **2002**, *71*, 989.
(4) Keese, R. *Chem. Rev.* **2006**, *106*, 4787.
(5) Merino, G.; Mendez-Rojas, M. A.; Vela, A.; Heine, T. *J. Comput. Chem.* **2007**, *28*, 362.
(6) Jemmis, E. D.; Jayasree, E. G.; Parameswaran, P. *Chem. Soc. Rev.* **2006**, *35*, 157.
(7) Radom, L.; Rasmussen, D. R. *Pure Appl. Chem.* **1998**, *70*, 1977.
(8) Monkhorst, H. *Chem. Commun.* **1968**, *18*, 1111.
(9) Hoffmann, R.; Alder, R. W.; Wilcox, C. F. *J. Am. Chem. Soc.* **1970**, *92*, 4992.
(10) Collins, J. B.; Dill, J. D.; Jemmis, E. D.; Apeloig, Y.; Schleyer, P. v. R.; Seeger, R.; Pople, J. A. *J. Am. Chem. Soc.* **1976**, *98*, 5419.
(11) Cotton, F. A.; Millar, M. *J. Am. Chem. Soc.* **1977**, *99*, 7886.
(12) Keese, R.; Pfenninger, A.; Roesle, A. *Helv. Chim. Acta* **1979**, *62*, 326.
(13) Boldyrev, A. I.; Simons, J. *J. Am. Chem. Soc.* **1998**, *120*, 7967.
(14) Gribanova, T. N.; Minyaev, R. M.; Minkin, V. I. *Collect. Czech. Chem. Commun.* **1999**, *64*, 1780.
(15) Li, X.; Wang, L. S.; Boldyrev, A. I.; Simons, J. *J. Am. Chem. Soc.* **1999**, *121*, 6033.
(16) Rasmussen, D. R.; Radom, L. *Angew. Chem., Int. Ed.* **1999**, *38*, 2876.
(17) Li, X.; Zhang, H. F.; Wang, L. S.; Geske, G. D.; Boldyrev, A. I. *Angew. Chem., Int. Ed.* **2000**, *39*, 3630.
(18) Wang, L. S.; Boldyrev, A. I.; Li, X.; Simons, J. *J. Am. Chem. Soc.* **2000**, *122*, 7681.
(19) Wang, Z. X.; Manojkumar, T. K.; Wannere, C.; Schleyer, P. v. R. *Org. Lett.* **2001**, *3*, 1249.
(20) Wang, Z. X.; Schleyer, P. v. R. *J. Am. Chem. Soc.* **2001**, *123*, 994.
(21) Wang, Z. X.; Schleyer, P. v. R. *J. Am. Chem. Soc.* **2002**, *124*, 11979.
(22) Merino, G.; Mendez-Rojas, M. A.; Vela, A. *J. Am. Chem. Soc.* **2003**, *125*, 6026.
(23) Sahin, Y.; Prasang, C.; Hofmann, M.; Subramanian, G.; Geiseler, G.; Massa, W.; Berndt, A. *Angew. Chem., Int. Ed.* **2003**, *42*, 671.
(24) Merino, G.; Mendez-Rojas, M. A.; Beltran, H. I.; Corminboeuf, C.; Heine, T.; Vela, A. *J. Am. Chem. Soc.* **2004**, *126*, 16160.
(25) Pancharatna, P. D.; Mendez-Rojas, M. A.; Merino, G.; Vela, A.; Hoffmann, R. *J. Am. Chem. Soc.* **2004**, *126*, 15309.
(26) Priyakumar, U. D.; Reddy, A. S.; Sastry, G. N. *Tetrahedron Lett.* **2004**, *45*, 2495.
(27) Esteves, P. M.; Ferreira, N. B. P.; Corroa, R. J. *J. Am. Chem. Soc.* **2005**, *127*, 8680.
(28) Gribanova, T. N.; Minyaev, R. M.; Minkin, V. I. *Russ. J. Gen. Chem.* **2005**, *75*, 1651.

"too small" to bind to all eight boron atoms simultaneously. However, a D_{8h} minimum could be realized if carbon is replaced by larger atoms, for example, boron and silicon in B_9^- and SiB_8,[41] respectively. This design followed the principles for achieving planar tetracoordinate main group element bonding laid out much earlier by Schleyer and Boldyrev.[50] This requires (1) a match in the radius of the outer ring and the size of the central atom (its "atomic radius") and (2) the presence of the appropriate number of valence electrons to occupy all binding molecular orbitals. Very recently, Wang and Boldyrev observed CB_7^- in the gas phase, which, however, corresponds to a global minimum with boron in center and the carbon in the outside ring.[51]

Although the violation of Kekule-van't Hoff-Lebel rules in species with planar hypercoordinate carbon seems unusual and intriguing, molecules containing other hypercoordinate elements are no less attractive. Bonačić-Koutecký et al. predicted the first example of a molecule containing planar hexacoordinate boron in 1991.[52] Further examples were reported subsequently.[53] Zhai et al. produced the planar hypercoordinate B_8^- and B_9^- boron anions by laser ablation and characterized them by photoelectron spectroscopy.[54] Their computational results suggested that the planarity of B_9^- is due to in-plane radial (p orbitals pointing toward the center of the boron ring) and π molecular orbitals (MOs). Furthermore, their theoretical results predicted the doubly aromatic character[55] arising from both the radial and π MOs. Later, Fowler and Gray carried out a detailed investigation of the MO symmetry and confirmed the double aromatic character of B_9^-.[56] Further examples of boron rings containing planar hypercoordinate atoms have been reported by Li et al.[29,57] and by Erhardt et al.[44] Planar hypercoordinate main group atoms centered in hexagonal hydrocopper complexes have been also proposed by Li et al.[58,59]

We now survey hypercoordinate group 14 elements at the center of *n*-membered boron rings ($n = 6$, 7, 8, 9, and 10) (*n*-MR). Boron clusters utilize extensively delocalized bonds readily. Due to its electron deficient character and propensity for deltahedral bonding, boron is intrinsically suitable for designing ring systems containing hypercoordinate elements. Our strategy for designing boron rings with planar hypercoordinate elements is based on the Schleyer-Boldyrev concepts.[50] First, the cyclic boron ligand must have the right size to accommodate a group 14 atom inside without steric repulsion. Second, the electronic structure of the molecule is adjusted by varying charge so that the molecule has six π and six radial electrons. We show here that successful applications of this strategy can extend the class of planar molecules containing group 14 elements with unusually high coordination.

II. Computational Details

The geometry optimizations and electronic structure calculations were performed with the B3LYP[60,61] functional as implemented in the Gaussian 03 program.[62] The 6-311+G(d) basis set[63] was used for C, Si, and Ge compounds. The def2-TZVPP basis set[64] with ECPs was used for those molecules containing Sn and Pb to take relativistic effects into account. Stationary points were characterized by harmonic frequency computations at the same theoretical levels. Zero-point energies were scaled by 0.9806 as recommended by Scott and Radom.[65] Wiberg bond indices (WBI)[66] were also computed. Potential energy surface scans for SiB_8 employed Saunders' stochastic search method.[67] As now implemented,[68] this method generates initial geometries randomly and processes them automatically. All atoms, placed at a same point initially, are displaced (kicked) randomly within a confined space. Two sets of 500 kick jobs were carried out in 2.5 and 4.0 Å cubic boxes. The initial structures were then optimized at the preliminary HF/STO-3G level. Redundant isomers (energies within 0.00001 a.u.) were discarded. The lowest energy isomers (within 0.1 Hartree of the best form) were further optimized at the B3LYP/6-311+G(d) level, followed by vibrational frequency computations.

While the induced magnetic field[69] ($\mathbf{B}^{ind}$) and the NICS[70,71] isosurfaces were performed using PW91[72] functional and IGLO-III[73] basis set for those planar local minima containing C and Si, computations for those minima containing Ge and Sn were calculated at PW91/DZVP[72,74] level. The shielding tensors were computed using the IGLO method.[75] The deMon program[76] was used to compute the molecular

(29) Li, S. D.; Guo, J. C.; Miao, C. Q.; Ren, G. M. *J. Phys. Chem. A* **2005**, *109*, 4133.
(30) Minyaev, R. M.; Gribanova, T. N.; Minkin, V. I.; Starikov, A. G.; Hoffmann, R. *J. Org. Chem.* **2005**, *70*, 6693.
(31) Su, M. D. *Inorg. Chem.* **2005**, *44*, 4829.
(32) Roy, D.; Corminboeuf, C.; Wannere, C. S.; King, R. B.; Schleyer, P. v. R. *Inorg. Chem.* **2006**, *45*, 8902.
(33) Wang, Y.; Huang, Y. H.; Liu, R. Z. *J. Mol. Struct.* **2006**, *775*, 61.
(34) Yang, L. M.; Ding, Y. H.; Sun, C. C. *J. Am. Chem. Soc.* **2007**, *129*, 1900.
(35) Yang, L. M.; Ding, Y. H.; Sun, C. C. *J. Am. Chem. Soc.* **2007**, *129*, 658.
(36) Perez, N.; Heine, T.; Barthel, R.; Seifert, G.; Vela, A.; Mendez-Rojas, M. A.; Merino, G. *Org. Lett.* **2005**, *7*, 1509.
(37) Li, S.-D.; Ren, G.-M.; Miao, C.-Q. *J. Phys. Chem.* **2005**, *109*, 259.
(38) Li, S.-D.; Ren, G.-M.; Miao, C.-Q.; Jin, Z.-H. *Angew. Chem., Int. Ed.* **2004**, *43*, 1371.
(39) Exner, K.; Schleyer, P. v. R. *Science* **2000**, *290*, 1937.
(40) Minyaev, R. M.; Gribanova, T. N.; Starikov, A. G.; Minkin, V. I. *Mendeleev Commun.* **2001**, 213.
(41) Wang, Z. X.; Schleyer, P. v. R. *Science* **2001**, *292*, 2465.
(42) Minyaev, R. M.; Gribanova, T. N.; Starikov, A. G.; Minkin, V. I. *Dokl. Chem.* **2002**, *382*, 41.
(43) Wang, Z. X.; Schleyer, P. v. R. *Angew. Chem., Int. Ed.* **2002**, *41*, 4082.
(44) Erhardt, S.; Frenking, G.; Chen, Z. F.; Schleyer, P. v. R. *Angew. Chem., Int. Ed.* **2005**, *44*, 1078.
(45) Wu, Y. B.; Yuan, C. X.; Yang, P. *THEOCHEM−J. Mol. Struct.* **2006**, *765*, 35.
(46) Ito, K.; Chen, Z. F.; Corminboeuf, C.; Wannere, C. S.; Zhang, X. H.; Li, Q. S.; Schleyer, P. v. R. *J. Am. Chem. Soc.* **2007**, *129*, 1510.
(47) Havenith, R. W. A.; Fowler, P. W.; Steiner, E. *Chem.−Eur. J.* **2002**, *8*, 1068.
(48) Li, S. D.; Miao, C. Q.; Ren, G. M.; Guo, J. C. *Eur. J. Inorg. Chem.* **2006**, 2567.
(49) Minyaev, R. M.; Gribanova, T. N. *Russ. Chem. Bull.* **2000**, *49*, 783.
(50) Schleyer, P. v. R.; Boldyrev, A. I. *J. Chem. Soc. Chem. Commun.* **1991**, 1536.
(51) Wang, L. M.; Huang, W.; Averkiev, B. B.; Boldyrev, A. I.; Wang, L. S. *Angew. Chem., Int. Ed.* **2007**, *46*, 4550.
(52) Bonacic-Koutecky, V.; Fantucci, P.; Koutecky, J. *Chem. Rev.* **1991**, *91*, 1035.
(53) Gu, T. L.; Yang, Z.; Tang, A.-C.; Jiao, H. J.; Schleyer, P. v. R. *J. Comp. Chem.* **1998**, *19*, 203.
(54) Zhai, H. J.; Alexandrova, A. N.; Birch, K. A.; Boldyrev, A. I.; Wang, L. S. *Angew. Chem., Int. Ed.* **2003**, *42*, 6004.
(55) Chandrasekhar, J.; Jemmis, E. D.; Schleyer, P. v. R. *Tetrahedron Lett.* **1979**, 3707.
(56) Fowler, P. W.; Gray, B. R. *Inorg. Chem.* **2007**, *46*, 2892.
(57) Li, S. D.; Miao, C. Q.; Guo, J. C.; Ren, G. M. *J. Am. Chem. Soc.* **2004**, *126*, 16227.
(58) Li, S. D.; Ren, G. M.; Miao, C. Q. *Inorg. Chem.* **2004**, *43*, 6331.
(59) Li, S. D.; Miao, C. Q. *J. Phys. Chem. A* **2005**, *109*, 7594.
(60) Becke, A. D. *J. Chem. Phys.* **1993**, *98*, 5648.
(61) Lee, C. T.; Yang, W. T.; Parr, R. G. *Phys. Rev. B* **1988**, *37*, 785.
(62) Frisch, G. W.; et al. *Gaussian 03*; Gaussian, Inc.: Pittsburgh, 2003.
(63) Krishnan, R.; Binkley, J. S.; Seeger, R.; Pople, J. A. *J. Chem. Phys.* **1980**, *72*, 650.
(64) Weigend, F.; Ahlrichs, R. *Phys. Chem. Chem. Phys.* **2005**, *7*, 3297.
(65) Scott, A. P.; Radom, L. *J. Phys. Chem.* **1996**, *100*, 16502.
(66) Wiberg, K. B. *Tetrahedron* **1968**, *24*, 1083.
(67) Saunders, M. *J. Comput. Chem.* **2004**, *25*, 621.
(68) Bera, P. P.; Sattelmeyer, K. W.; Saunders, M.; Schaefer, H. F.; Schleyer, P. v. R. *J. Phys. Chem. A* **2006**, *110*, 4287.
(69) Merino, G.; Heine, T.; Seifert, G. *Chem.−Eur. J.* **2004**, *10*, 4367.
(70) Schleyer, P. v. R.; Maerker, C.; Dransfeld, A.; Jiao, H. J.; Hommes, N. J. R. V. *J. Am. Chem. Soc.* **1996**, *118*, 6317.
(71) Chen, Z. F.; Wannere, C. S.; Corminboeuf, C.; Puchta, R.; Schleyer, P. v. R. *Chem. Rev.* **2005**, *105*, 3842.
(72) Perdew, J. P.; Wang, Y. *Phys. Rev. B* **1992**, *45*, 13244.
(73) Kutzelnigg, W.; Fleischer, U.; Schindler, M. *The IGLO-Method: Ab Initio Calculation and Interpretation of NMR Chemical Shifts and Magnetic Susceptibilities*; Springer-Verlag: Heidelberg, 1990; Vol. 23.

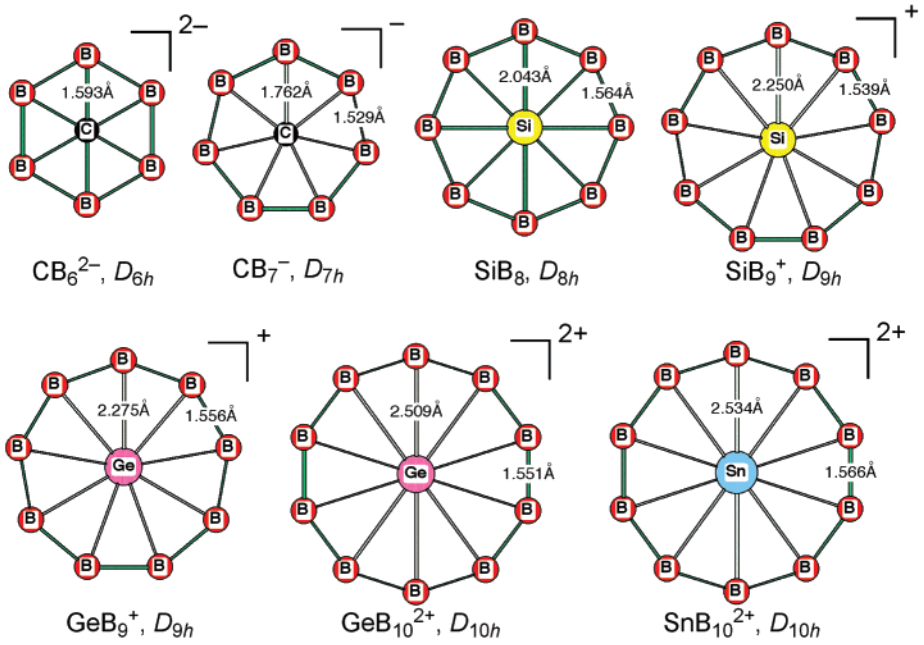

Figure 1. Optimized geometries of planar boron wheels containing a planar hypercoordinate group 14 element. Bond distances are given in Å.

orbitals and the deMon-NMR package[77] for the shielding tensors. Induced magnetic fields were computed in ppm of the external field applied perpendicular to the molecular plane. Assuming an external magnetic field of $|\mathbf{B}^{ext}| = 1.0$ T the unit of $\mathbf{B}^{ind}$ is 1.0 μT, which is equivalent to 1.0 ppm of the shielding tensor. To render the induced magnetic fields the molecules were oriented so that the center of mass located at the origin of the coordinate system; the *z*-axis is parallel to the highest order symmetry axis of the molecule. The external field is applied perpendicular to the molecular plane. The σ and π contributions to the induced magnetic field[78] and the NICS function have been separated using the IGLO method, where localized molecular orbitals (LMOs) have been created using the procedure suggested by Pipek and Mezey.[79] In addition, out-of-plane (zz) tensor component (in ppm) contribution from individual canonical molecular orbital to NICS (CMO−$NICS_{zz}$)[80−82] are computed at PW91/def-TZVPP level to evaluate the behavior of the radial and π MOs using NBO 5.0.[83] VU[84] was employed for the visualization of molecular fields.[85]

III. Results and Discussion

All the minima containing a planar hypercoordinate group 14 element at the center of various sizes of boron rings are depicted in Figure 1. The design strategy discussed above is general and works well with the boron ring sizes from 6 to 10, and the central group 14 elements from carbon to tin.

AB_6^{2-} Structures. The singlet D_{6h} CB_6^{2-},[39] reported previously, has equal C−B and B−B lengths (1.593 Å; see Table 1 for geometrical parameters), which are in the ranges of C−B and B−B covalent bond distances.[86] However, the B_6 ring is too small to accommodate the heavier carbon congeners. For

Table 1. Point Groups (PG), A−B Bond Distances (r_{AB}, in Å), HOMO−LUMO Gap (Gap in eV), Number of Imaginary Frequencies (NIMG), the Smallest Vibrational Frequencies (ν_{min}, in cm^{-1}), and Relative Energies with Respect to Minima (ΔE, in kcal·mol^{-1}), Including Zero Point Energy of $AB_n^{(8-n)a}$

	PG	r_{AB}	Gap	NIMG	$\nu_{min.}$	ΔE
CB_6^{2-}	D_{6h}	1.593	2.2	0	269.7	−
SiB_6^{2-}	D_{6h}	1.794	2.08	2	362.1*i*	122.1
GeB_6^{2-}	D_{6h}	1.858	1.49	2	424.4*i*	183.2
SnB_6^{2-} (T)	D_{6h}	2.16	2.33	6	559.1*i*	241.4 (T)
PbB_6^{2-} (T)	D_{6h}	2.229	2.14	6	562.8*i*	271.8 (T)
CB_7^-	D_{7h}	1.762	3.79	0	54.7	−
SiB_7^-	D_{7h}	1.889	3.57	1	228.7*i*	8.5
GeB_7^-	D_{7h}	1.939	3.59	1	195.1*i*	28.5
SnB_7^-	D_{7h}	2.052	3.38	1	233.3*i*	159.2 (T)
PbB_7^-	D_{7h}	2.102	2.89	1	222.0*i*	217.3 (T)
CB_8	D_{8h}	2.03	3.53	2	513.3*i*	14.7
SiB_8	D_{8h}	2.043	3.62	0	65.9	−
GeB_8	D_{8h}	2.08	3.75	1	73.4*i*	0.9
SnB_8	D_{8h}	2.157	3.73	1	168.6*i*	35.3
PbB_8	D_{8h}	2.197	3.39	1	173.1*i*	111.7 (T)
CB_9^+	D_{9h}	2.223	2.53	6	528.6*i*	43.5
SiB_9^+	D_{9h}	2.25	3.26	0	134.9	−
GeB_9^+	D_{9h}	2.275	3.41	0	105.5	−
SnB_9^+	D_{9h}	2.322	3.41	1	83.1*i*	3.7
PbB_9^+	D_{9h}	2.354	3.18	1	107.4*i*	16
CB_{10}^{2+}	D_{10h}	2.487	1.54	8	468.3*i*	74.4
SiB_{10}^{2+}	D_{10h}	2.495	2.84	2	73.5*i*	−0.3[b]
GeB_{10}^{2+}	D_{10h}	2.509	2.77	0	100.2	−
SnB_{10}^{2+}	D_{10h}	2.534	2.99	0	57.9	−
PbB_{10}^{2+}	D_{10h}	2.556	2.86	1	37.0*i*	0.5

[a] All species are singlets unless indicated to be triplets (T). [b] Although D_{10h} SiB_{10}^{2+} has two in-plane degenerate imaginary frequencies, which distort to C_{2v} SiB_{10}^{2+}, C_{2v} geometry is slightly less stable than D_{10h} if the scaled ZPE correction is applied.

(74) Godbout, N.; Salahub, D. R.; Andzelm, J.; Wimmer, E. *Can. J. Chem.* **1992**, *70*, 560.
(75) Kutzelnigg, W. *Isr. J. Chem.* **1980**, *19*, 193.
(76) Koster, A. M.; Geudtner, G.; Goursot, A.; Heine, T.; Vela, A.; Patchkovskii, S.; Salahub, D. R. *deMon 2001*; NRC: Canada, 2002.
(77) Malkin, V. G.; Malkina, O. L.; Salahub, D. R. *Chem. Phys. Lett.* **1993**, *204*, 80.
(78) Heine, T.; Islas, R.; Merino, G. *J. Comput. Chem.* **2007**, *28*, 302.
(79) Pipek, J.; Mezey, P. G. *J. Chem. Phys.* **1989**, *90*, 4916.
(80) Corminboeuf, C.; Heine, T.; Seifert, G.; Schleyer, P. v. R.; Weber, J. *Phys. Chem. Chem. Phys.* **2004**, *6*, 273.
(81) Heine, T.; Schleyer, P. v. R.; Corminboeuf, C.; Seifert, G.; Reviakine, R.; Weber, J. *J. Phys. Chem. A* **2003**, *107*, 6470.
(82) Fallah-Bagher-Shaidaei, H.; Wannere, C. S.; Corminboeuf, C.; Puchta, R.; Schleyer, P. v. R. *Org. Lett.* **2006**, *8*, 863.
(83) Reed, A. E.; Curtiss, L. A.; Weinhold, F. *Chem. Rev.* **1988**, *88*, 899.
(84) Ozell, B.; Camarero, R.; Garon, A.; Guibault, F. *Finite Elem. Des.* **1995**, *19*, 295.
(85) Merino, G.; Vela, A.; Heine, T. *Chem. Rev.* **2005**, *105*, 3812.
(86) The reference covalent bond distances are as follows: CH_3BH_2 (C_s), 1.554; SiH_3BH_2 (C_s), 2.017; GeH_3BH_2 (C_s), 2.066; SnH_3BH_2 (C_s), 2.258; PbH_3BH_2 (C_s), 2.304; B_2H_4 (D_{2d}), 1.629; B_2H_2 (D_{8h}), 1.507 Å. CH_3BH_2, SiH_3BH_2, GeH_3BH_2, B_2H_4, and B_2H_2 geometries are optimized at B3LYP/6−311++G** level, and SnH_3BH_2 and PbH_3BH_2 geometries were optimized at B3LYP/def2-TZVPP level. For additional covalent bond distance reference, see Suresh, C. H.; Koga, N. *J. Phys. Chem. A* **2001**, *105*, 5940.

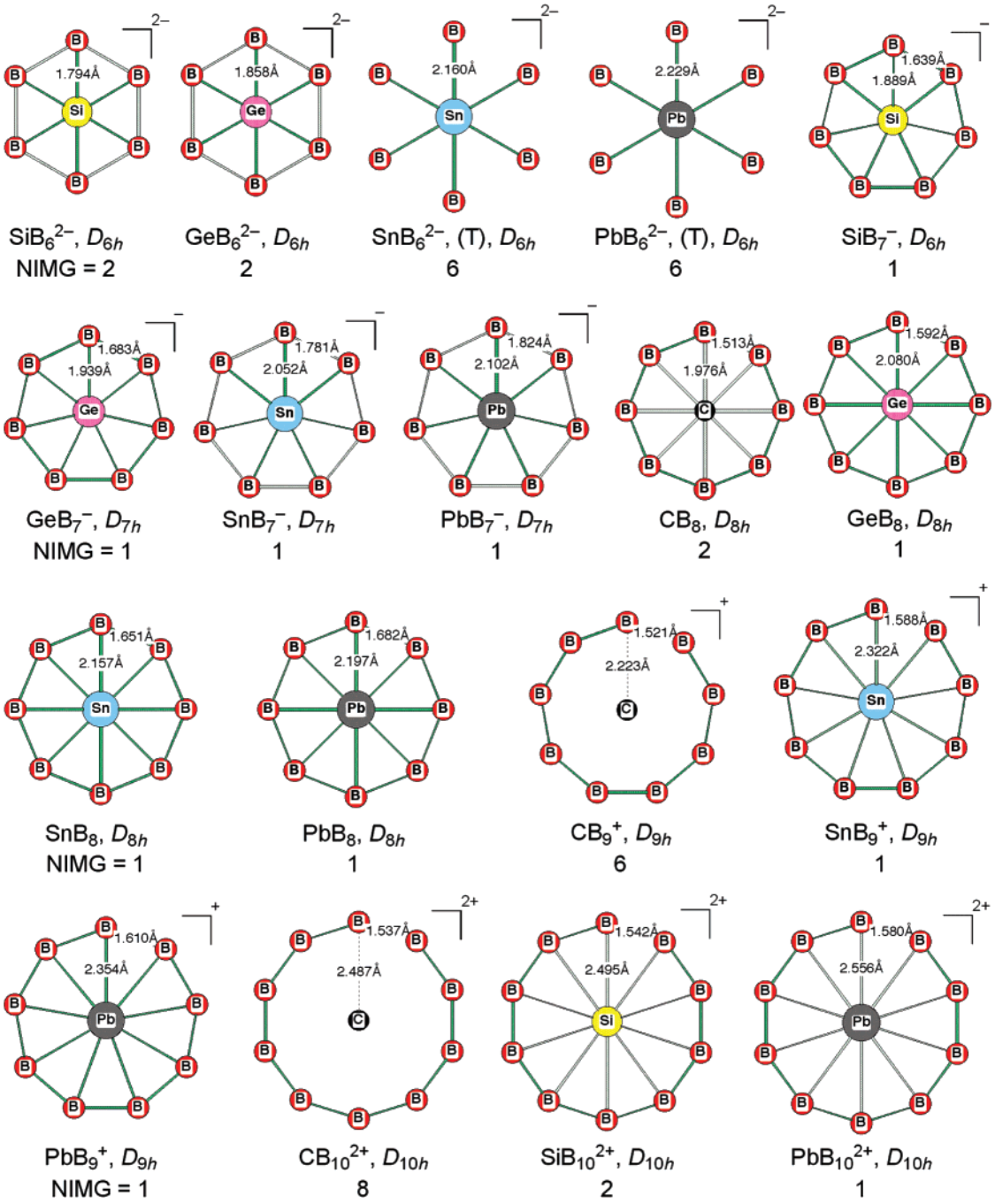

Figure 2. Optimized geometries of boron rings saddle points with hypercoordinate group 14 elements. Bond distances are in Å.

example, D_{6h} symmetry SiB_6^{2-} and GeB_6^{2-} (see Figure 2) structures have two imaginary frequencies: one out-of-plane and one in-plane (D_{6h} to D_{3h}) deformations. Following the out-of-plane imaginary mode results in distorted pyramidal C_{2v} SiB_6^{2-} (see Figure 3) and C_{2v} GeB_6^{2-}, which are 122.1 and 183.2 kcal·mol^{-1} lower in energy compared to D_{6h} SiB_6^{2-} and GeB_6^{2-}, respectively. Unlike D_{6h} SiB_6^{2-} and GeB_6^{2-}, D_{6h} SnB_6^{2-} and PbB_6^{2-} (see Figure 2) have triplet ground states.[87]

In D_{6h} SnB_6^{2-} and PbB_6^{2-}, the tin and lead atoms are too large to fit inside of the B_6 ring cavity, and D_{6h} SnB_6^{2-} and PbB_6^{2-} have six imaginary frequencies in D_{6h} symmetry. Further optimization in lower symmetries results in a C_{3v} pyramidal structure. The triplet C_{3v} SnB_6^{2-} and PbB_6^{2-} are more stable than their planar geometries by 241.4 and 271.8 kcal·mol^{-1}, respectively. The increasing stabilization due to pyramidalization (122.1 for SiB_6^{2-} to 271.8 kcal·mol^{-1} in PbB_6^{2-}; see Table 1) is consistent with the increasing size of the central atoms. This reveals the importance of the geometrical fit for designing stable boron rings with planar hypercoordinate elements.

AB_7^- Structures. Although the D_{7h} CB_7^- is a minimum, the 7-MR is still too small to incorporate heavier group 14 elements: D_{7h} AB_7^- (A = Si, Ge, Sn, Pb; see Figure 2) are

(87) When compared to a hypothetical model of D_{6h} SnB_6^{2-} with short Sn-B distance (constrained to 1.8 Å), a highly unfavorable anti-bonding B−B interaction (b_{1u} MO; see Figure 1-SI) are now reduced due to the long B−B distance in triplet D_{6h} SnB_6^{2-}. Meanwhile, bonding e_{1g} π MOs become less stable due to the increased B−B distance, resulting in the inversion of occupied (e_{1g}) and the unoccupied (b_{1u}), so that b_{1u} MO is fully occupied, leaving degenerate e_{1g} π MOs singly occupied. Hence, SnB_6^{2-} and, similarly, PbB_6^{2-} are triplet ground states.

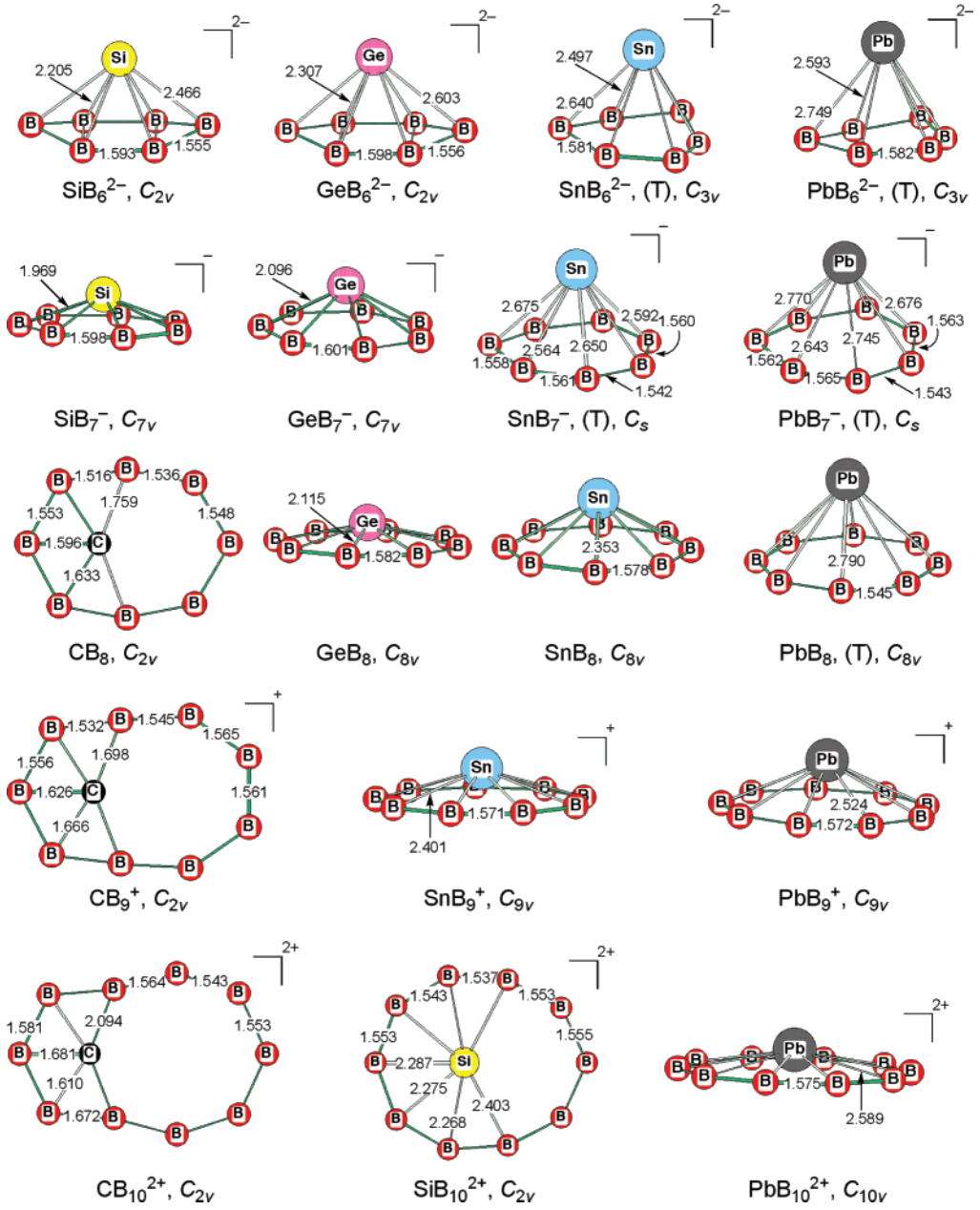

Figure 3. Fully optimized geometries of minima shown in Figure 2. Bond distances are in Å.

transition states associated with movement of the central atom out of the ring plane. The A−B lengths are too short (Table 1) compared to a covalent A−B bond distances so that pyramidal distortion occurs. The resulting singlet pyramidal C_{7v} SiB_7^- and GeB_7^- (see Figure 3) are 8.6 and 28.5 kcal·mol^{-1} more stable than the planar structure, respectively (Table 1). On the other hand, pyramidal C_s SnB_7^- and PbB_7^- (see Figure 3) are triplet ground states[88] and are 159.2 and 217.3 kcal·mol^{-1} more stable than singlet planar D_{7h} geometries, respectively (see Figure 2).

Neutral AB_8 Structures. Our calculations show that planar D_{8h} CB_8 is a second-order saddle point. As found earlier,[41] the B_8 ring is too large to accommodate a carbon in the center (distortion to planar pentacoordinate carbon structures (C_{2v}, CB_8) occurs; see Figure 3), but a silicon atom is accommodated comfortably, resulting in D_{8h} SiB_8 (see Figure 1). The Si−B bond length in the D_{8h} SiB_8 is 2.043 Å, within a reasonable covalent Si−B distance.[86] On the other hand, the planar hypercoordinate structures for heavier group 14 congeners are transition states for the pyramidalization. In GeB_8, the pyramidal distortion is so small that the C_{8v} minimum GeB_8 is almost planar (see Figure 3). In fact, C_{8v} GeB_8 is only 0.9 kcal·mol^{-1} lower in energy than D_{8h} planar geometry. The pyramidal C_{8v} minimum of SnB_8 (Figure 3) is 35.3 kcal·mol^{-1} lower in energy than the D_{8h} planar geometry. The triplet ground-state C_{8v} PbB_8 minimum (Figure 3) is 111.7 kcal·mol^{-1} lower in energy than the singlet D_{8h} planar geometry (Figure 2).

AB_9^+ Structures. As expected, D_{9h} CB_9^+ is not a minimum; it has six imaginary frequencies. Like CB_8, the central carbon atom moves to the edge to form a planar pentacoordinate carbon minimum (Figure 3). However, the D_{9h} planar nonacoordinate

(88) In SnB_7^-, PbB_7^-, and PbB_8, the anti-bonding a_1 interaction is diminished as the central atom moves away from the B_n rings, whereas radial bonding e_1 MO interactions become less stable, resulting in the inversion of a_1 and e_2 MOs (see Figure 2-SI). Hence, a_1 MO is fully occupied and e_2 MOs are singly occupied in SnB_7^-, PbB_7^-, and PbB_8.

Table 2. A−B and Total Wiberg Bond Indices (WBI_{A-B} and $WBI_{Tot.}$, Respectively) of D_{nh} Planar Boron Ring Minima with Hypercoordinate Atoms[a]

	WBI_{A-B}	$WBI_{Tot.}$
1	0.64	3.84
2	0.56	3.92
3	0.47	3.79
4	0.41	3.67
5	0.41	3.67
6	0.33	3.30
7	0.33	3.31

[a] Computations were carried out at B3LYP/6-311+G* for $CB_n^{(n-8)}$, $SiB_n^{(n-8)}$, and $GeB_n^{(n-8)}$ and B3LYP/def2-TZVPP for $SnB_n^{(n-8)}$ and $PbB_n^{(n-8)}$.

species with silicon and germanium are minima. The A−B distances in D_{9h} SiB_9^+ and GeB_9^+ are 2.250 and 2.275 Å, respectively (Figure 1). The smallest vibrational frequencies (134.9 for D_{9h} SiB_9^+ and 105.5 cm^{-1} for D_{9h} GeB_9^+), which correspond to central atom movements out of the ring plane, are appreciable. On the other hand, tin and lead atoms are too large to fit inside the B_9 ring cavity: the D_{9h} SnB_9^+ and PbB_9^+ are transition states. Following the imaginary vibrational frequency results in the pyramidal C_{9v} SnB_9^+ and PbB_9^+ (see Figure 3), which are 3.7 and 16.0 kcal·mol^{-1} lower in energy compared to the planar D_{9h} geometries, respectively.

AB_{10}^{2+} Structures. The same approach can be used for designing planar decacoordinate AB_{10}^{2+} structures. The B_{10} cavity in CB_{10}^{2+} and SiB_{10}^{2+} is too large for a carbon or silicon atom to bind strongly to all 10 boron atoms simultaneously; D_{10h} CB_{10}^{2+} has eight imaginary frequencies. Further optimization results in the more stable C_{2v} planar pentacoordinate carbon minimum (Figure 3) by 74.3 kcal·mol^{-1} compared to D_{10h} geometry. The D_{10h} SiB_{10}^{2+} has two degenerate imaginary frequencies and results in C_{2v} SiB_{10}^{2+} (Figure 3). However, when scaled ZPE correction is included, D_{10h} SiB_{10}^{2+} is more stable than C_{2v} SiB_{10}^{2+} by only 0.3 kcal·mol^{-1}. Hence, SiB_{10}^{2+} is essentially planar. A 10-membered ring is the best choice to fit a germanium or a tin atom, resulting in D_{10h} GeB_{10}^{2+} and SnB_{10}^{2+} (see Figure 1). The A−B interatomic distances are 2.509 and 2.534 Å for D_{10h} GeB_{10}^{2+} and SnB_{10}^{2+}, respectively, in these beautiful structures. Although D_{10h} PbB_{10}^{2+} has one imaginary frequency, which deforms to pyramidal C_{10v} geometry, pyramidal distortion is very small and C_{10v} PbB_{10}^{2+} is nearly planar (Figure 3). In fact, C_{10v} geometry is only 0.5 kcal·mol^{-1} lower in energy than the D_{10h} structure.

Bond Order Analysis. The A−B bond distances in the planar CB_7^-, SiB_9^+, GeB_9^+, GeB_{10}^{2+}, and SnB_{10}^{2+} are significantly longer than comparable covalent bond distances.[86] However, A−B Wiberg bond indices (WBI) show the A−B bond order ranges from 0.64 in D_{6h} CB_6^{2-} to 0.33 in D_{10h} SnB_{10}^{2+} (see Table 2), indicating significant A−B bonding interactions. The total WBI of the central atom range from 3.8 for D_{6h} CB_6^{2-} to 3.3 for D_{10h} SnB_{10}^{2+}, which indicates that each A−B bond is weak, but the number of A−B binding compensates for the weak A−B bonding interactions. However, the octet rule is not violated despite the hypercoordination.

Molecular Orbital Analysis. Although the size of the boron ring is a key factor in achieving planar D_{nh} AB_n molecules, the proper electronic "fit" is also essential for their stability. Like B_8^- and B_9^- (B_9^- is valence isoelectronic with the AB_8 species where A = C, Si, Ge, Sn, and Pb),[54] planarity of the hypercoordinate boron systems is achieved due to the stabilization of extensively delocalized six π and six radial electrons. Figure 4 shows plots of both the π and the radial MOs of $AB_n^{(n-8)}$ (n = 6−10). The six π electrons in π_0 and the degenerate π_1 MOs are extensively delocalized. Although the central atoms have an appreciable p_z coefficient in the π_0 MO, the nodal planes of the degenerate π_1 orbitals (HOMOs) through the center atom preclude the bonding of the central element to the peripheral boron atoms. The six radial electrons in Rad_0 and the degenerate Rad_1 MOs are appreciably delocalized as well and are used effectively to help bind the central element to the cyclic boron ligand. The lowest radial MO (Rad_0) bond with the s orbital of the central atom, whereas the next higher laying radial MOs interacts favorably with the p_x and p_y orbitals of the central atom, resulting in (Rad_1) radial MOs. The efficient use of six radial electrons may be as important in planarizing such boron wheel molecules as the six π electrons.

Magnetic Properties. The appreciable delocalization of both π and radial MOs of the hypercoordinate species described above results in magnetic aromaticity, as shown by our computations of the induced magnetic field and NICS. For example, the total response of the induced magnetic fields and their σ- and π-separated z-components of D_{8h} SiB_8, which coincide with the $NICS_{zz}$ index,[80] are plotted in Figure 5a. Like benzene, the total response is strongly diatropic (shown in red) inside the main ring (Figure 5a). However, both σ and π-components of SiB_8 contribute strongly, indicating its doubly aromatic character. This behavior is similar to that observed previously for Al_4^{2-} and boron rings.[56,89−91] The directly related NICS isosurfaces also were computed (Figure 5b). Like $\mathbf{B}^{ind}$, the NICS values inside the boron rings are strongly diatropic (red). However, the NICS value at the central atom is paratropic (blue). Similar magnetic response is observed for all title compounds (see Figures 3-SI and 4-SI).

Dissection of the out-of-plane tensor component of $NICS(1)_{zz}$ (NICS probe placed at 1.0 Å above the central atom) into contributions from each canonical molecular orbital (CMO−$NICS(1)_{zz}$, see Figure 6) of D_{8h} SiB_8 shows that the sum of the contribution for the radial MOs ($NICS_{Rad.} = -30.3$, see Figure 6) are as large as that of π contribution ($NICS_{\pi} = -29.5$) indicating the doubly aromatic character of D_{8h} SiB_8. Similar CMO−$NICS(1)_{zz}$ trends were observed in CB_6^{2-}, CB_7^-, and GeB_9^+ (see Figures 5-SI, 6-SI, and 7-SI, respectively). The large $NICS(1)_{zz}$ contribution from the radial MOs indicates the importance of the radial MOs in stabilizing these molecules.

These results are in complete agreement with the conclusions drawn from the MO analysis, showing that extensive delocalization is a key factor for the stabilization of the boron wheels containing a hypercoordinate group 14 element.

Viability. Although the structures and hypercoordinate bonding of all these hypercoordinate group 14 minima are exciting, their kinetic also must be evaluated. Are these novel boron ring molecules viable chemically? Can they be produced and characterized, for example, in the gas phase or in matrix isolation, if not in solution or in bulk? Are other minima lower in energy?

(89) Li, X.; Kuznetsov, A. E.; Zhang, H. F.; Boldyrev, A. I.; Wang, L. S. *Science* **2001**, *291*, 859.
(90) Islas, R.; Heine, T.; Merino, G. *J. Chem. Theory Comput.* **2007**, *3*, 775.
(91) Chen, Z. F.; Corminboeuf, C.; Heine, T.; Bohmann, J.; Schleyer, P. v. R. *J. Am. Chem. Soc.* **2003**, *125*, 13930.

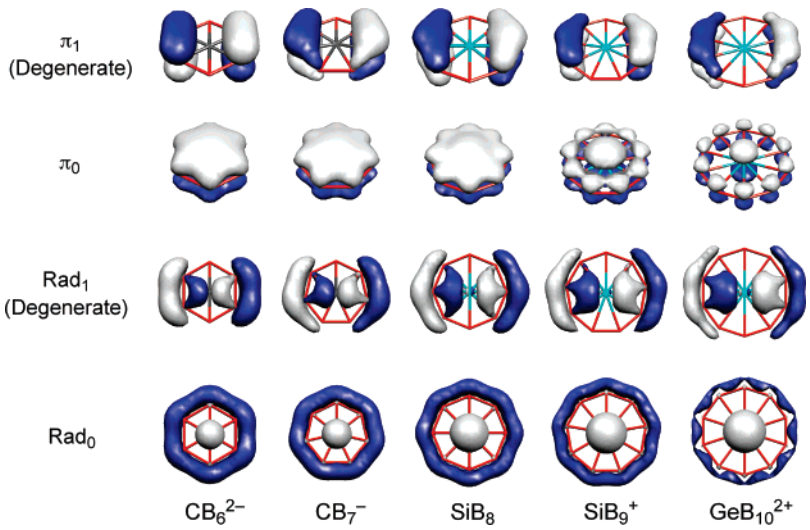

Figure 4. Occupied π and radial molecular orbitals of selected planar hypercoordinate systems. π_0 is the lowest π MO, π_1 is the degenerate second lowest π MO, Rad_0 is the the lowest radial MO, and Rad_1 is the the degenerate second lowest radial MO.

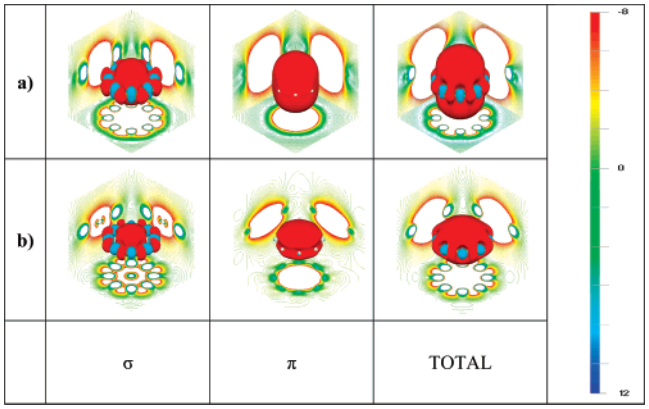

Figure 5. Isosurfaces and contour lines of (a) z component of $\mathbf{B}^{ind}$ and (b) NICS of D_{8h} SiB_8. $|\mathbf{B}_z^{ind}| = 8\ \mu T$ and $\mathbf{B}^{ext} = 1$ T. $\mathbf{B}^{ind}$ and NICS computations were performed at PW91/IGLO-III level.

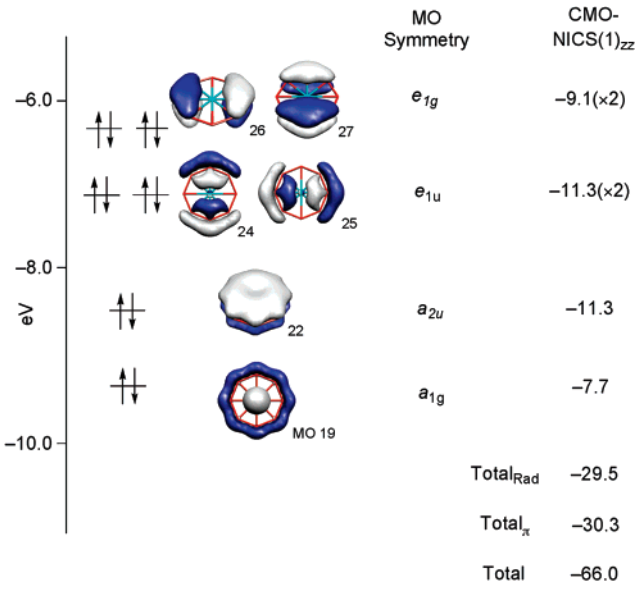

Figure 6. CMO−NICS(1)$_{zz}$ of D_{8h} SiB_8 computed at PW91/def-TZVPP level. $Total_{Rad}$ and $Total_{\pi}$ are the sum of contributions from all radial and π MOs, respectively. Total value includes contributions from σ, radial, π, and core electrons.

The recent experimental and theoretical study of CB_7^- by Boldyrev and Wang[51] illustrates these concerns. Instead of having a heptacoordinate carbon, their evidence pointed to a CB_7^- C_{2v} structure, with a planar heptacoordinate boron at the ring center and the carbon in the outside ring.

We emphasize that the existence of more stable nonplanar or other isomers does not preclude the possibility of producing and observing planar hypercoordinate molecules. Rather, the viability of planar centrosymmetric carbon species depends on their kinetic stability, which, if high enough, may enable their preparation and characterization under different experimental conditions, even if other isomers are lower in energy. Furthermore, planar hypercoordination is intriguing, whatever element is involved.

We chose D_{8h} SiB_8 as an example for detailed examination here. Despite the normally weaker Si−B bond energies, the thermodynamic stability of D_{8h} SiB_8 is documented by its large atomization energy per atom of 4.29 eV. This is comparable to that of the experimentally produced B_9^-(4.71 eV), as well as the 4.69 eV for the most stable planar (C_{2v}) "carbon outside" form of CB_8.[41] In addition, the HOMO−LUMO gap of D_{8h} SiB_8 (3.62 eV) is substantial and resembles that of B_9^- and CB_8 (3.82 and 3.74 eV, respectively). The appreciable vertical ionization and vertical attachment energies of D_{8h} SiB_8 (8.62 and 1.54 eV, respectively) are also similar to the "carbon outside" C_{2v} CB_8 (8.36 and 1.11 eV, respectively).

We carried out a potential energy surface scan using the stochastic search Kick method[68] to search for SiB_8 isomers. The results, summarized in Figure 7, show that only one minimum is more stable than the D_{8h} geometry, although the energy difference is appreciable. The global minimum has C_{7v} symmetry with the silicon atom occupying the axial position of a heptagonal bipyramid, whereas the D_{8h} isomer with an octacoordinate silicon is 33.3 kcal/mol higher in energy. However, our extensive searches for transition states from the planar D_{8h} to the heptagonal bipyramidal C_{7v} have not located any direct reaction path between the D_{8h} and the C_{7v} isomer. Indeed, the kinetic stability of all planar minima with hypercoordinate group 14 species were analyzed by simulated annealing techniques, involving density-functional Born−Oppenheimer molecular dynamics calculations at the PBE/DZVP level. At a simulated temperature of 600 K, all the boron wheel minima in Figure 1

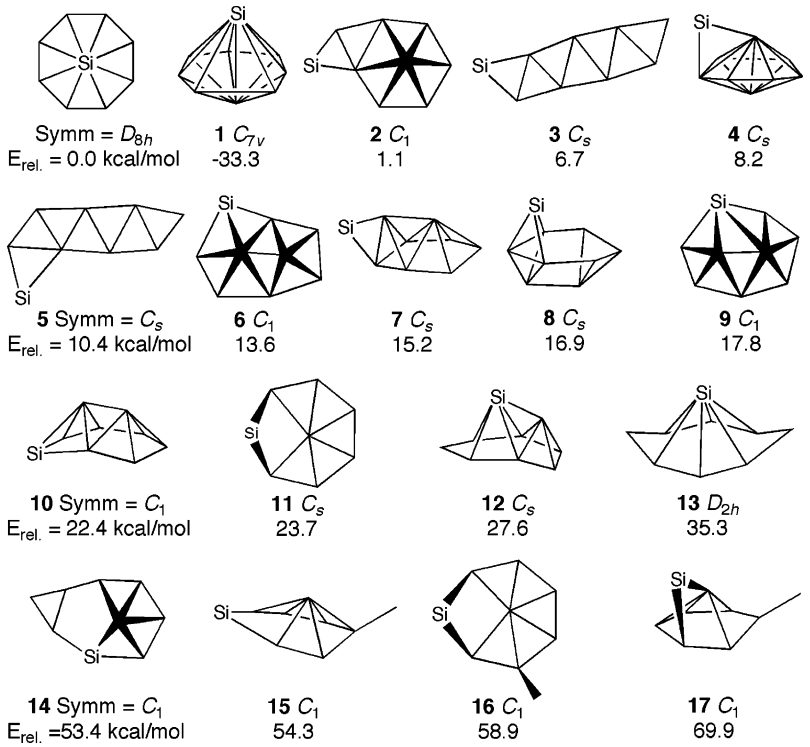

Figure 7. Stationary points of SiB_8 calculated with B3LYP/6-311+G*. E_{rel} is the energy difference of the corresponding structure minus that containing a planar octacoordinate silicon, including the scaled ZPE.

retained their topologies during 5 ps equilibration and 10 ps propagation times. As these calculations turned out to be rather computationally expensive, longer-time-scale simulations were not affordable. Moreover, the CB_7^- preference for hypercoordinate boron[51] does not apply to SiB_8. The C_{2v} SiB_8 isomer with the silicon on the outside ring is a second-order saddle point. Further optimization results in C_s isomer (**11** in Figure 7) with the silicon atom out of plane. The C_s isomer is 26.2 kcal·mol^{-1} higher in energy than the symmetric D_{8h} SiB_8.

IV. Conclusions

We illustrate that a rational strategy can be employed to design boron wheels containing hypercoodinate group 14 elements (C, Si, Ge, Sn, and Pb) in their centers. The ring and group 14 atomic radii must match. In addition, the radial/π electron delocalization determines the stability of these hypercoordinate molecules. Both of those requirements are important factors for the planarization for these molecules for the D_{nh} molecules ranging from CB_6^{2-} to SnB_{10}^{2+} in Figure 1. No planar center symmetric lead analogs were located within the scope of our study. CB_6^{2-}, CB_7^-, SiB_8, and GeB_9^+ were characterized by MO analysis, induced magnetic field computations, and CMO−NICS to be doubly aromatic. Although individual bonds from ring boron atoms to the central atom may be relatively weak, their unusually large number results in stability of the planar hypercoordinate molecules.

SiB_8 was studied in more detail. A PES scan using the Kick method revealed only one C_{7v} isomer to be more stable than D_{8h} form, albeit by over 33.3 kcal·mol^{-1}. However, the D_{8h} form was found to be kinetically viable by Born−Oppenheimer molecular dynamics computation. Life times of at least 10 ps of planar hypercoordinate minimum of SiB_8, as well as the other planar minima in Figure 1, show the feasibility of their gas-phase production and characterization. The prediction that such novel molecules with planar hypercoordinate group 14 element are viable offers many opportunities for experimental realization since their barriers to isomerization appear to be very high.

Acknowledgment. We dedicate this paper to Roald Hoffmann on the occasion of his 70th birthday. We thank him, along with Alberto Vela and Miguel Angel Mendez-Rojas for cheerful discussions. We gratefully acknowledge support from AMC-ACS-Fomex, DINPO, DFG, and NSF (CHE-0716718). Invaluable technical help was provided by Ariana Teissier. R.I. acknowledges Conacy for a Ph.D. fellowship.

Note Added after ASAP Publication: In the version published November 6, 2007, Roald Hoffmann's name was misspelled. It has been corrected for the print and online publications.

Supporting Information Available: Complete author list for ref 62. The MO plots, the isosurfaces and contour lines of the induced magnetic field and NICS computations, and the CMO−$NICS(1)_{zz}$ results. Cartesian coordinates (in Å) and total energies of all compounds discussed in the text. This material is available free of charge via the Internet at http://pubs.acs.org.

JA074956M